



HAL
open science

OFDM signal down frequency conversion based on a SOA-MZI sampling mixer using differential modulation and switching architectures

Hassan Termos, Ali Mansour

► **To cite this version:**

Hassan Termos, Ali Mansour. OFDM signal down frequency conversion based on a SOA-MZI sampling mixer using differential modulation and switching architectures. *Optik*, 2021, 245, pp.167761. 10.1016/j.ijleo.2021.167761 . hal-03327443

HAL Id: hal-03327443

<https://ensta-bretagne.hal.science/hal-03327443v1>

Submitted on 8 Feb 2023

HAL is a multi-disciplinary open access archive for the deposit and dissemination of scientific research documents, whether they are published or not. The documents may come from teaching and research institutions in France or abroad, or from public or private research centers.

L'archive ouverte pluridisciplinaire **HAL**, est destinée au dépôt et à la diffusion de documents scientifiques de niveau recherche, publiés ou non, émanant des établissements d'enseignement et de recherche français ou étrangers, des laboratoires publics ou privés.



Distributed under a Creative Commons Attribution - NonCommercial 4.0 International License

OFDM signal down frequency conversion based on a SOA-MZI sampling mixer using differential modulation and switching architectures

Hassan Termos, Ali Mansour

Lab STICC, ENSTA Bretagne, 2 Rue François Verny, 29806 Brest Cedex 9, France

A simulation performance analysis of a semiconductor optical amplifier Mach–Zehnder inter-ferometer (SOA-MZI) sampling mixer used as a frequency down converter is presented by employing differential modulation and switching architectures. A clock pulse signal, generating 2 ps-width pulses at a sampling frequency of 13 GHz, is used as a sampling signal. Two optical carriers, intensity-modulated by a sinusoidal signal at 79 and 80 GHz are simultaneously down converted to 1 and 2 GHz, respectively. For the differential modulation architecture, conversion gains of about 34 and 32 dB are demonstrated for the frequency down conversion to 1 and 2 GHz, respectively. Besides, the conversion gain of 20 dB is achieved for down conversion from 79 to 1 GHz for the differential switching architecture. Furthermore, signals modulated by an orthogonal frequency division multiplexing (OFDM) complex modulation format at different bit rates are also down converted from 79 to 1 GHz and from 80 to 2 GHz and their error vector magnitude (EVM) is evaluated and compared. A maximum bit rate of about 8 Gbps satisfying the forward error correction (FEC) limit is fulfilled using differential modulation and switching architectures.

1. Introduction

Radio over Fiber (RoF) systems have attracted significant attention by enabling the transmission of frequency mixing of optical fiber signals. Such systems enjoy the advantages of low loss transmission, low weight, wide bandwidth and being immunity to electromagnetic interference. There are numerous of RoF applications such as cellular or satellite communications, wireless fidelity (WiFi), and radar systems [1]. Different techniques to implement mixed optical signals have been studied to enhance the performance of a RoF system and minimize the system cost based on a SOA-MZI [2–6] and other optical mixers [7–14]. Frequency converters play a pivotal role in all-optical architectures by providing switching functions. Among frequency converter approaches, semiconductor optical amplifier Mach–Zehnder interferometers (SOA-MZIs), which equally exploit the nonlinear phenomena of XGM (Cross-Gain Modulation) and XPM (Cross-Phase Modulation), are used for frequency mixing [2–5]. This optical mixer has received essential attention thanks to their high performance, stability, and potential for integration with other optical devices. Sampling methods recently became the most effective techniques to improve the characteristics of an optical transmission system. A SOA-MZI, used as a sampling mixer to perform frequency mixing in standard and differential modes [5], is an integrated all-optical switch. SOA-MZI provides large extinction ratio while lowering the required optical input power due to its interferometric structure [5] compared to other optical mixers. In our previous work, an optical transmission system based on a SOA-MZI differential mode [5,15] reported conversion gain for multiple mixing frequencies. Specifically, an optical signal at 39.5 GHz is down converted at a frequency of 26.5 GHz related to the first harmonic of the sampling signal, and 0.5 GHz related third harmonic of the sampling signal. The down conversion gain obtained at the

mixing frequency of 0.5 GHz is 18.1 dB [15].

Recently, a theoretical and experimental analysis of the performance of the modulation architecture of a SOA-MZI sampling mixer used for frequency up conversion purposes are presented [16]. In the experimental part, an up conversion gain equal to 9 dB is achieved for the 1 GHz to 39 GHz conversion when employing the modulation architecture. The conversion of complex-modulated data signals has also been realized by the photonic microwave mixer. The EVM values of sampled QPSK signal are considerably improved by using the technique of the modulation architecture. Besides, the bit rate can attain up to 1 Gbps.

In this paper, we use a differential modulation architecture to accomplish simultaneous frequency mixing based on the SOA-MZI sampling mixer by using a Virtual Photonics Integrated (VPI) simulator. The highest conversion gain is reached with the differential modulation architecture based on the SOA-MZI sampling mixer for frequency down conversion of an optical signals from 79 to 1 GHz and 80 to 2 GHz, simultaneously, which are related to the sixth harmonic of the sampling signal. Moreover, we evaluate the quality of the frequency down conversion system using orthogonal frequency division multiplexing (OFDM) complex modulated signals, which are done for the first time for the differential modulation architecture. We have compared its performance in terms of the conversion gain and error vector magnitude (EVM) against the established differential switching architecture, both based on the SOA-MZI photonic sampler. The remainder of the paper is arranged as follows. In Section II, we describe the principle of operation for the differential modulation and switching architectures. In Section III, the conditions of the conducted simulations are analyzed and

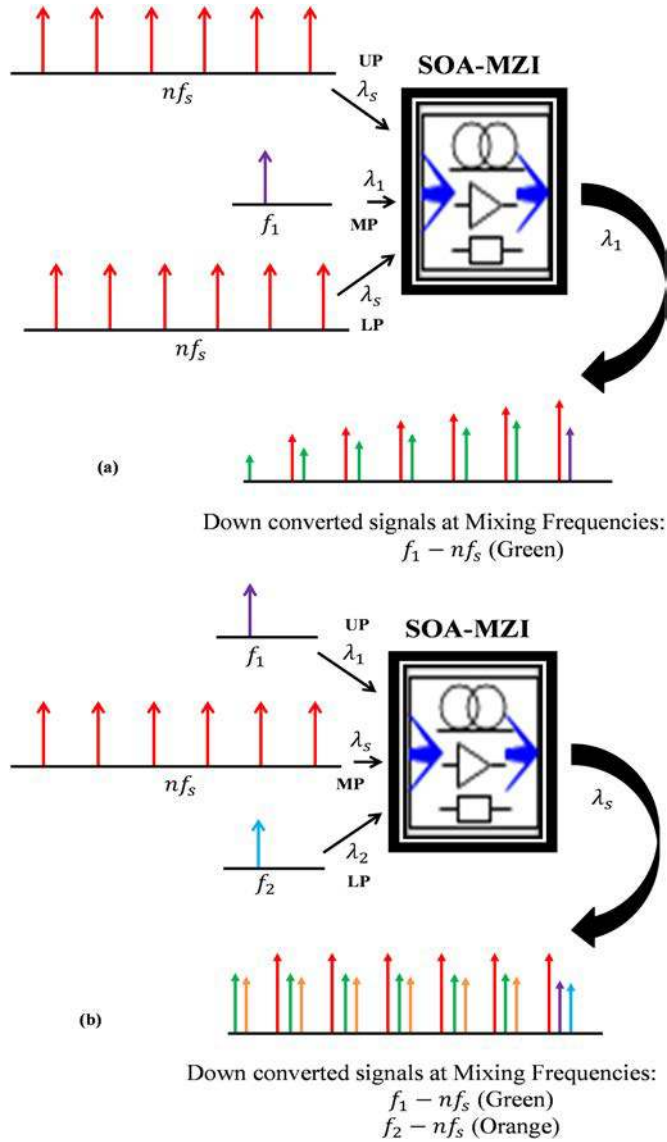


Fig. 1. SOA-MZI differential switching architecture (a). The data signals at frequencies f_1 and f_2 are down converted at mixing frequencies $f_1 - nf_s$ and $f_2 - nf_s$, respectively. SOA-MZI differential modulation architecture (b). The data signal at f_1 is down converted at $f_1 - nf_s$. n varies from one to six in this work. MP: Middle Port, LP: Lower Port, and UP: Upper Port.

simulation conversion gain results are given for both principles. In Section IV, the simulation results for the frequency down conversion of complex-modulated OFDM data by the differential switching and modulation architectures against the EVM are presented. Last and not least, in Section V, the conclusions reached through this work are given.

2. Principle of differential modulation and switching architectures

The principle of differential switching architecture already explained in [5,15] is displayed in Fig. 1(a). The sampling signal at a frequency f_s is injected at the upper and lower ports while the one at the upper port (UP) is slightly delayed compared to the one applied at the lower port (LP). On the other hand, the data signal at a carrier frequency f_1 is entered at the middle port (MP) and split into the upper and lower arms. The data signal is switched on and off by the sampling signal. This configuration, which actively turns off the SOA-MZI used as an optical switch [17], leads to a reduced transmission time window. Hence, the data signal is down converted at the mixing frequencies $f_1 - nf_s$ as seen in the electrical spectrum at the SOA-MZI output.

The proposed differential modulation architecture, which is done for the first time to the best of our expertise, is depending on a cross phase modulation (XPM) of two input optical signals in the MZI built using SOAs as shown in Fig. 1(b). In this architecture, the incoming data signals are launched into the two SOAs where they modulate the gain of the SOAs, which their carrier density as well as their refractive index are modulated, and thereby the gain and phase of the sampling signal. In other words, the sampling signal is modulated by the data signals. This sampling signal that corresponds to ultra-short clock pulses with a sampling frequency f_s , at the wavelength λ_s is coupled into the MP of the MZI and split into upper and lower arms at the same time by using an optical coupler. The data signals at the carrier frequencies f_1 and f_2 are injected at the UP and LP, respectively. The presence of the data signal affects the phase of the sampling signal due to the XPM. Then, a phase shift occurs on the sampling signal in the upper arm, while another phase shift appears on the same signal in the lower arm. Thus, this causes a phase modulation of the sampling signal propagating in the SOAs according to the input data signals. At the output of the interferometer, the signal from the two SOAs interferes in order to obtain the sampled signal. This signal is well improved at the SOA-MZI output due to enhance the amplified sampling signal that maintains the same power of its harmonics whatever the harmonic rank is. As we can see from the electrical spectrum of the sampled signal obtained after optical filtering centered at λ_s , the data signals are down converted from f_1 to $f_1 - nf_s$ and from f_2 to $f_2 - nf_s$, where n is the harmonic rank of the sampling signal that ranges from 1 to 6. The differential modulation architecture achieves two things together: firstly the improvement of the down converted signal at the SOA-MZI output and simultaneous frequency down conversion of two radio frequency (RF) signals.

3. Simulation setup

The simulation setup proposed to fulfill the differential modulation architecture is described in Fig. 2. Firstly, the current of both SOAs is adopted to be the same, i.e. 380 mA. This value helps to acquire a more stable response of the SOA-MZI. Furthermore, the wavelength of the signal injected at SOA-MZI middle port is $\lambda_s = 1550$ nm and the ones injected at input upper and lower ports are chosen to be λ_1 at 1545 nm and λ_2 at 1547 nm, respectively. Finally, the mean optical powers of the signal at upper and lower ports are -12 and -15 dBm, respectively. An optical pulse clock (OPC) source is driven at a sampling frequency f_s equal to 13 GHz and gives

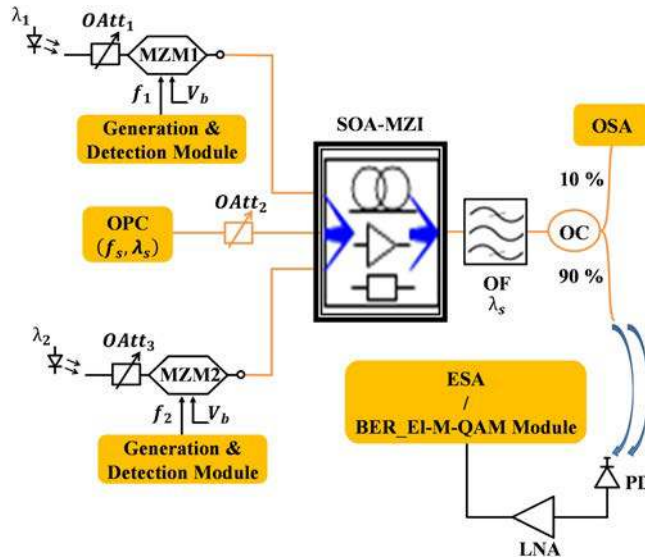


Fig. 2. Simulation setup for the differential modulation architecture. OAtt: Optical Attenuator. MZM: Mach-Zehnder Modulator. OF: Optical Filter. LNA: Low Noise Amplifier. OSA: Optical Spectrum Analyzer. ESA: Electrical Spectrum Analyzer, QAM: Quadratic Amplitude Modulation, OC: Optical Coupler, and OPC: Optical Pulse Clock.

an optical pulse train of 2 ps full-width at half-maximum pulses. The optical power of the sampling signal injected at the SOA-MZI middle port is varied from -10 to 6 dBm.

The center frequency of the optical filter (OF) placed at the SOA-MZI output is tuned at 1550 nm to select the sampled signal produced by the interferometer, while removing the optical data signals. The OF bandwidth is chosen to be 0.7 nm in order to filter the amplified spontaneous emission (ASE) noise while permitting the harmonics needed for the range of 80 GHz of the frequency down conversion technique to travel. At the upper and lower ports, the data signals, which are to be down converted at the SOA-MZI output, are produced by continuous wave (CW) laser sources, which are intensity modulated by optical MZMs stimulated by the generation and detection module at $f_1 = 79$ GHz and $f_2 = 80$ GHz, respectively. This module at the electrical port of the MZM is used to manufacture the sine wave signal for down conversion gain measurements and the OFDM signals for EVM ones.

The RF signals are then frequency converted around the harmonics of OPC source. The sampled signal emerging from the SOA-MZI output is optically filtered by the OF. The filtered optical signal can also be monitored and displayed in an optical spectrum analyzer (OSA) using $90/10$ optical coupler (OC) through its 10% port. The sampled signal at the 90% port of the OC, is then photo-detected by a 100 GHz PIN photodiode whose responsivity is 0.82 A/W. The electrical output signal is then amplified by a 33 -dB low noise amplifier (LNA). Afterwards, this amplified signal is displayed on an electrical spectrum analyzer (ESA) to achieve the frequency down conversion spectrum, which includes the harmonics of the sampling signal, the amplified data signals, and the down converted replicas, in order to calculate the down conversion gain or used the BER_EL-M-QAM module to demodulate the OFDM data and calculate its EVM.

In Fig. 3, the SOA-MZI is used in a differential switching architecture where the data signal at f_1 is used at the MP and the sampling signal at f_s is injected at the UP and LP. The wavelength of the data signal is $\lambda_1 = 1545$ nm and its optical mean power is -12 dBm. The setup includes now a variable optical delay line (VODL) used to adjust the relative delay of 10 ps of the control pulses between the UP and LP. The relative power between these ports is controlled by Att1 and Att3. The down converted signal at the SOA-MZI output is now filtered at λ_1 . It is worth noting all the other parameters are the same in Figs. 2 and 3. Besides, the most important SOA parameters are shown in Table 1.

The real SOA-MZI used in our simulations by the VPI simulator is shown in Fig. 4. It is used to obtain a frequency conversion to lower frequencies and simultaneous two RF signals to be down converted by all-optical sampling, while its static and dynamic characteristics are studied in order to identify the best operating point used in the frequency down conversion process. This SOA-MZI is used for the differential mode in the modulation and switching architectures.

The nominal operating point is chosen to obtain a minimum transmission, i.e.: both SOAs are both biased at 350 mA and the phase shifter is tuned in order to control the minimum optical power at the SOA-MZI output when the command signal at the input control port is null. The operating point has been selected to maximize the extinction ratio (ER) at the SOA-MZI output.

The data signal having a mean optical power of -12 dBm at the wavelength of 1545 nm is injected into the input data port. The wavelength of the sampling signal at the upper port is 1550 nm. Fig. 5 displays the static characteristic of the SOA-MZI with a maximum ER = 35.5 dB. It is observed that the maximum transmitted powers of the data signal at the SOA-MZI output is achieved at the optical power of -1 dBm at the input control port.

The carrier's lifetime and recombination time play a role on the dynamic behavior of the SOA-MZI [18]. In order to improve its dynamic behavior, a SOA must be biased with a high bias current, which corresponds to 350 mA for both SOAs. A constant optical power of -12 dBm at the wavelength of 1545 nm is injected at the input data port and an intensity-modulated optical power of -1 dBm at 1550 nm is infused at the control port. At the SOA-MZI output, the modulated optical data signal is photo-detected and amplified. Its frequency response in Fig. 4 conveys a low-pass behavior with a 8.2 GHz cutoff frequency (Fig. 6).

To validate the approach of the differential modulation architecture at the SOA-MZI output, the electrical spectrum is displayed at this port after photo-detection and amplification as illustrated in Fig.7. The two RF original signals are down converted at the mixing

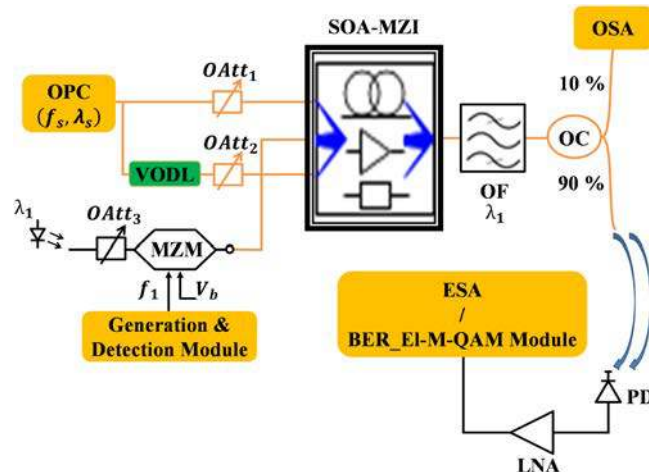


Fig. 3. Differential switching architecture setup of the all-optical sampling mixer. VODL: Variable Optical Delay Line.

Table 1
The SOAs parameter value used in the simulation SOA-MZI setup.

Parameter	Value	Unit
Linewidth enhancement factor	4	
Differential Carrier Lifetime	27	ps
Carrier Lifetime	70	ps
SOA Saturation Power	15	dBm
SOA1 Gain	26	dB
SOA2 Gain	28	dB

frequencies $|f_m + nf_s|$ at the SOA-MZI output. There are twenty four down converted signals at different mixing frequencies ranging from $f_2 - f_s = 67$ GHz to $|f_1 - 12f_s| = 77$ GHz in Fig. 7. Besides, we can observe that the frequency down converted signals involve up to the twelfth harmonic of the sampling signal. As mentioned in the approach, the harmonics maintain the same power. However, in reality the harmonics degrade slightly with the frequency. The difference between the first and the sixth harmonic is about 4 dB due to the SOA-MZI low pass behavior. This leads to increase the replicas of the sampled signal because they follow the harmonics of the sampling signal. It worth noting that the difference between the down converted signal at $f_m - f_s$ and the one at $f_m - 6f_s$ is about 6 dB. Moreover, simultaneous down conversion of two RF signals are also achieved at the SOA-MZI output.

In Fig. 8, we exhibit the electrical spectrum of down converted signals at the SOA-MZI output for the differential switching architecture. As explained in the approach, the replicas of the sampled signal decrease with the mixing frequency because they follow the harmonics of the sampling signal and due to the SOA-MZI low pass behavior. The difference between the down converted signal at $f_1 - f_s$ and the one at $f_1 - 6f_s$ is about 15 dB, which is higher than the difference between the same range for the differential modulation architecture. As a result, the differential modulation architecture improves extremely the characteristics of the down converted signals, especially at the higher mixing frequencies as illustrated in Fig. 8.

4. Conversion gain

In order to quantify the performances of the sampling mixer based on the differential modulation architecture, the electrical conversion gain is assessed. It is defined as the difference between the electrical power in dBm provisioned at the SOA-MZI output at mixing frequencies $|f_m - nf_s|$ and the electrical power in dBm referenced at the SOA-MZI inputs at f_m , where m is an integer value. The simulations are carried out by using a virtual photonic integrated (VPI) Transmission Maker [19].

In Fig. 9, the conversion gain is obtained at the SOA-MZI output at $f_1 - 6f_s = 1$ GHz and $f_2 - 6f_s = 2$ GHz for distinct optical powers of the sampling signal driven by the OPC source at the middle port of the SOA-MZI. The maximum conversion gains are attained at the optical power of -1 dBm. Their values are 34 and 32 dB at the mixing frequency of 1 and 2 GHz, respectively.

The down conversion gain is also obtained versus the mixing frequency for differential switching and modulation architectures as displayed in Fig. 10. For channel one that is the RF signal at $f_1 = 79$ GHz, it ranges from 39 dB at the mixing frequency $f_1 - f_s = 66$ GHz relevant to the first harmonic of the sampling signal to 34 dB at $f_1 - 6f_s = 1$ GHz related to the sixth harmonic. Besides, it degrades 2 dB over the entire mixing frequency for channel two that is the RF signal at $f_2 = 80$ GHz for the differential modulation architecture. Furthermore, the difference between the conversion gain at $f_1 - f_s = 66$ GHz and the one at $f_1 - 6f_s = 1$ GHz is 15.5 dB for the differential switching architecture. As a result, the differential modulation principle improves the conversion gain about 14 dB at $f_1 - 6f_s = 1$ GHz compared to the conversion gain at the same frequency for the differential modulation principle.

In the experimental work based on the SOA-MZI differential switching configuration, the down conversion gain of 18.1 dB was obtained at 0.5 GHz related to the fifth harmonic of the sampling signal $5f_s = 39$ GHz [15], which is close to the conversion gain of 20 dB at 1 GHz related to the sixth harmonic of the sampling signal $6f_s = 78$ GHz for the simulation work based on the VPI simulator. For this work, we have interchanged the sinusoidal signal with the sampling signal driven by the OPC source at the SOA-MZI inputs so that the frequency components that participate in the f_m to $f_m - 6f_s$ frequency conversion are not filtered for the differential modulation architecture as $f_k - 6f_s$ lies inside the XPM bandwidth, which is the cutoff frequency $f_c = 8.2$ GHz. On the other hand, the high harmonic $6f_s$ of the sampling signal maintains approximately the close electrical power to the first harmonic. This explains the increased robustness of the differential modulation scheme with respect to the conversion gain as the down conversion frequency decreases. Hence, the effect of each critical SOA-MZI parameter depends in any case on the exact operating point of the SOA-MZI.

5. Down conversion of complex-modulated data simulation results

A frequency down mixing of OFDM data carried by the electrical subcarrier at the electrical port of the optical MZMs is evaluated for diverse bit rates (BRs) at the SOA-MZI output. A generation and detection module generates OFDM data at the carrier frequency f_m . This module brings about the same quality of the data signal injected at the upper and lower arms with different frequencies.

The error vector magnitude (EVM) [20] of the down converted signals at the SOA-MZI output is assessed in order to study the quality of the frequency mixing based on the differential modulation architecture. The EVM of the sampled signals has been obtained through the BER_EI-M-QAM module. As in VPI's demo, this module is handled to evaluate the EVM of the received constellation. This metric is related to the Bit Error Rate (BER), and the acceptable limit is defined as the value that provides an equivalent BER of 0.0038, which guarantees error free performance after applying forward error correction (FEC) techniques [21].

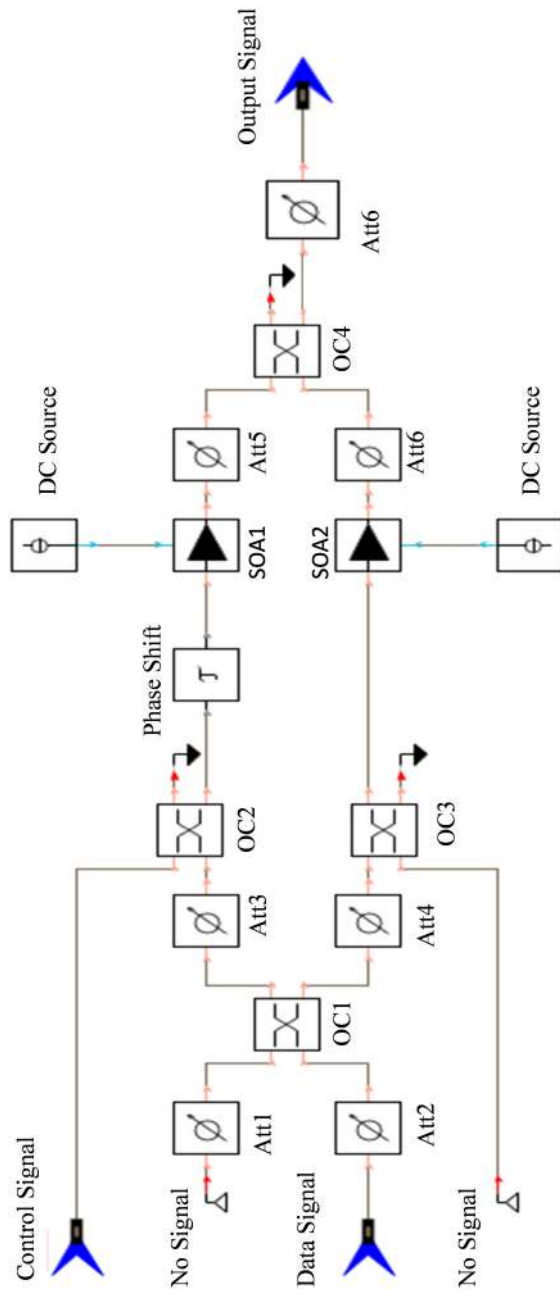


Fig. 4. SOA-MZI Schematic used in the VPI simulator: Att: Attenuator, OC: Optical Coupler, and SOA: Semiconductor Optical Amplifier.

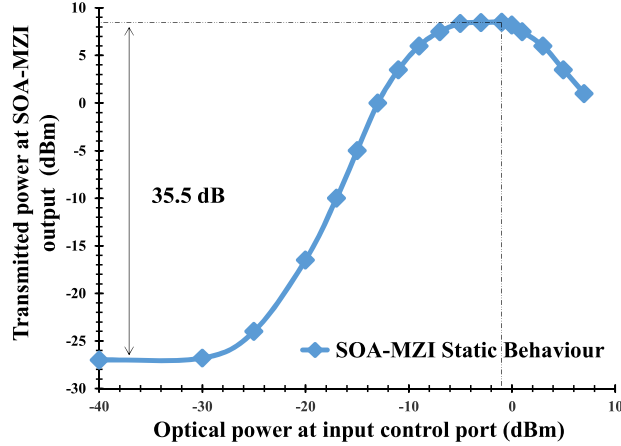


Fig. 5. SOA-MZI static characteristic used in the VPI simulation setup with ER = 35.5 dB.

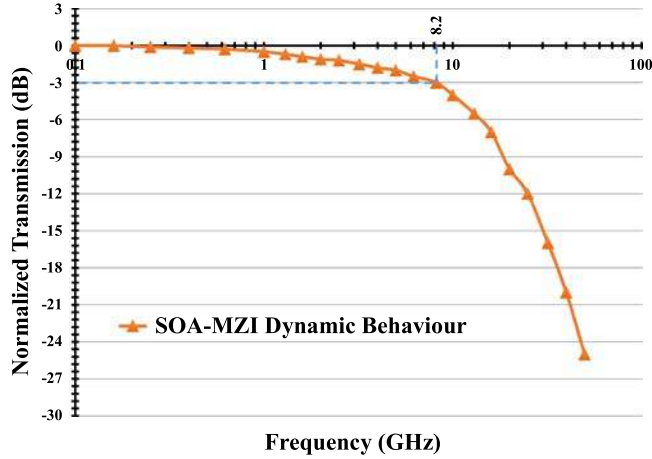


Fig. 6. SOA-MZI dynamic behavior with the cutoff frequency of 8.2 GHz.

The OFDM data description is considered and studied in [22]. In our work, 64 subcarriers are used to generate the transmitted OFDM data at the carrier frequency f_m . Besides, the cyclic prefix (CP) of 25% is fixed. Using the differential modulation architecture, we can perform frequency down conversion at high harmonics up to $12f_s$ without significant degradation of the down converted signals quality.

In Fig. 11, for OFDM-modulated data, a bit rate of 8 Gbps is achieved for frequency down conversions from 79 to 1 GHz and from 80 to 2 GHz when applying the differential modulation architecture. The EVM augments with the bit rate. It reaches 15 and 17 % at the mixing frequencies of 1 and 2 GHz, respectively, at BR = 8 Gbps. However, the EVM for differential switching architecture is higher at the higher mixing frequencies. It reaches 28 % at 1 GHz at BR = 8 Gbps, which is 13 % higher compared to the differential modulation at the same mixing frequency and bit rate. On the other hand, our experimental works of the differential switching performance deteriorate rapidly as the bit rate increases, reaching the EVM of 15 % for the conversion towards 0.5 GHz at BR = 163.84 Mbps [22]. As a result, maintaining the power of the harmonics of the sampling signal improves the quality of the optical transmission system for the differential configuration.

6. Conclusion

In this manuscript and based on the differential modulation and switching architectures, we recommend a pioneer work related to the frequency down conversion system using orthogonal frequency division multiplexing (OFDM) complex modulated signals. We have granted an analysis of the performance of the differential modulation and switching architectures of a SOA-MZI sampling mixer used for frequency down conversion purposes. Our results show a conversion gain equal to 34 dB for the 79 to 1 GHz conversion, while a conversion gain equal to 32 dB is attained for the 80 to 2 GHz conversion when employing the differential modulation architecture. For the differential switching architecture, the conversion gain reaches 20 dB at the mixing frequency of 1 GHz. The difference between

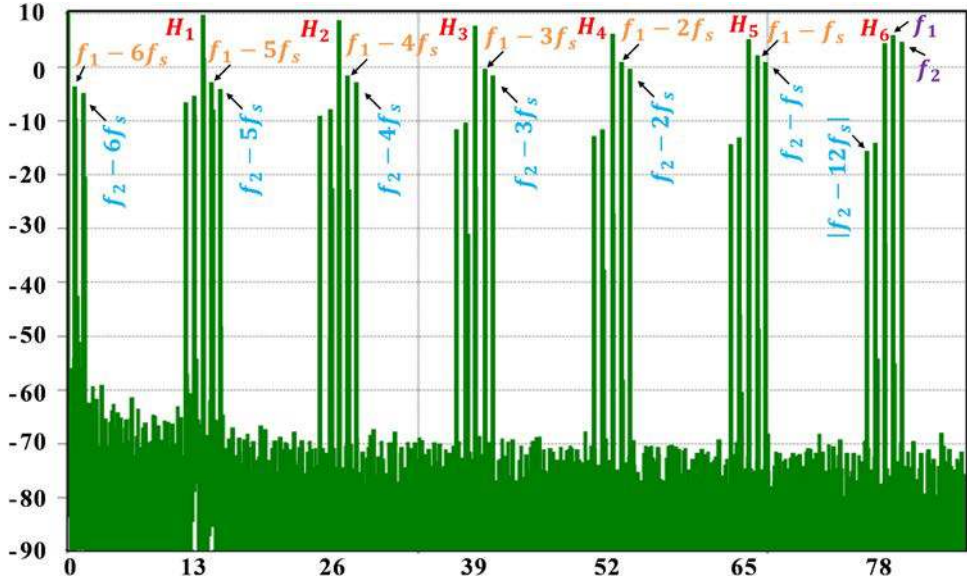


Fig. 7. Electrical spectrum of the sampled signal at mixing frequencies $|f_m - nf_s|$ at the SOA-MZI output for the differential modulation architecture, where m and n are an integer. The source frequencies at the SOA-MZI input is $f_1 = 79$ GHz and $f_2 = 80$ GHz, the sampling frequency is $f_s = 13$ GHz and the harmonics of the sampling signal are at $H_n = nf_s$, and mixing frequencies are $|f_m - nf_s|$. m ranges from 1 to 2 and n ranges from 1 to 6.

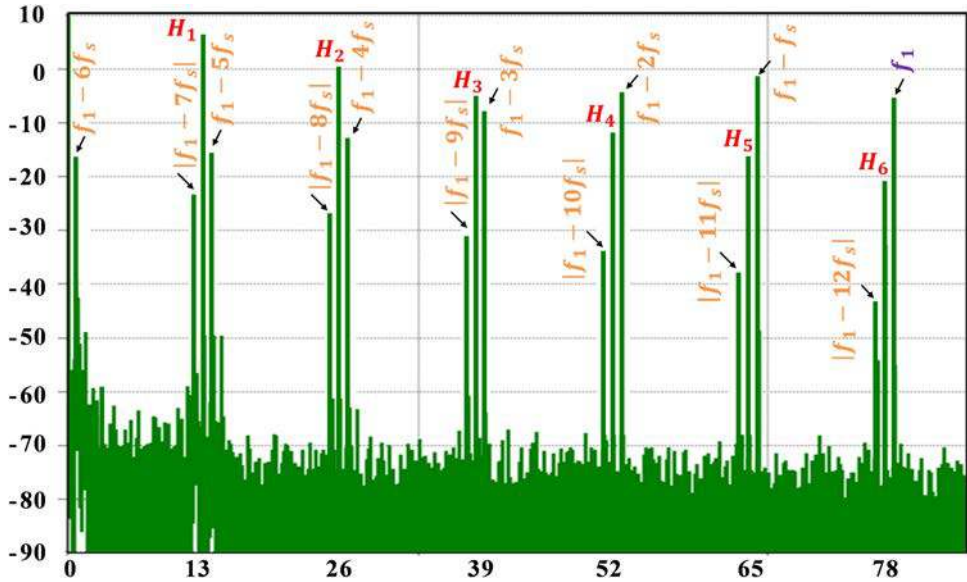


Fig. 8. Electrical spectrum of the sampled signal at mixing frequencies $|f_1 - nf_s|$ at the SOA-MZI output for the differential switching architecture. The source frequency at the SOA-MZI input is $f_1 = 79$ GHz, the sampling frequency is $f_s = 13$ GHz and the harmonics of the sampling signal are at $H_n = nf_s$, and mixing frequencies are $|f_1 - nf_s|$. The n value ranges from 1 to 6.

the simultaneous down converted signal results for the conversion gain is 2 dB over the entire range of the optical input powers of the sampling signal and the mixing frequencies. The conversion of complex-modulated data signals has also been realized by the sampling mixer. We have thus obtained a sufficiently low EVM for OFDM modulations when applying the differential modulation architecture for both 79 to 1 GHz and 80 to 2 GHz frequency conversion at the higher bit rate. This allows to support a data bit rate equal to 8 Gbps. The differential modulation improves the efficiency through the conversion gain of 14 dB at 1 GHz and the quality through the EVM of 13 % at 1 GHz at BR = 8 Gbps of the optical transmission system compared to the differential switching.

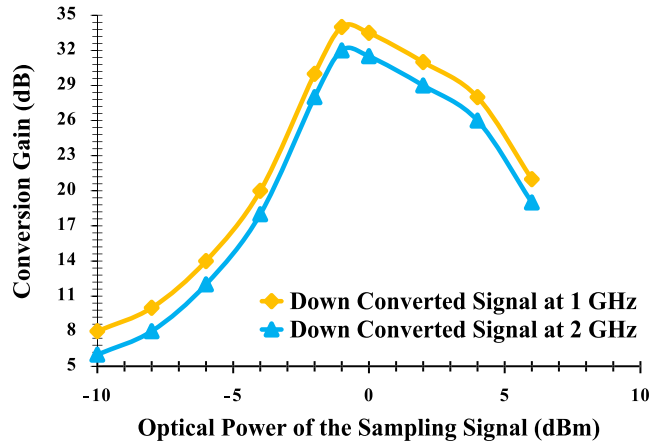


Fig. 9. Comparison between conversion gains for two down converted signals at the SOA-MZI output at $f_1 - 6f_s = 1$ GHz and $f_2 - 6f_s = 2$ GHz based on the differential modulation architecture.

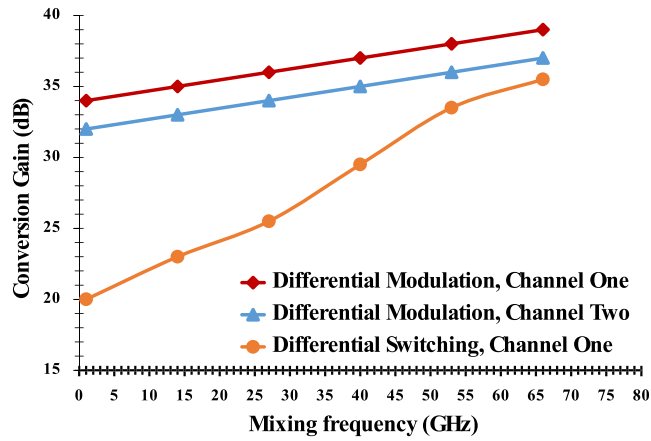


Fig. 10. Conversion gains of down converted signals for differential modulation and switching architectures as a function of the mixing frequency.

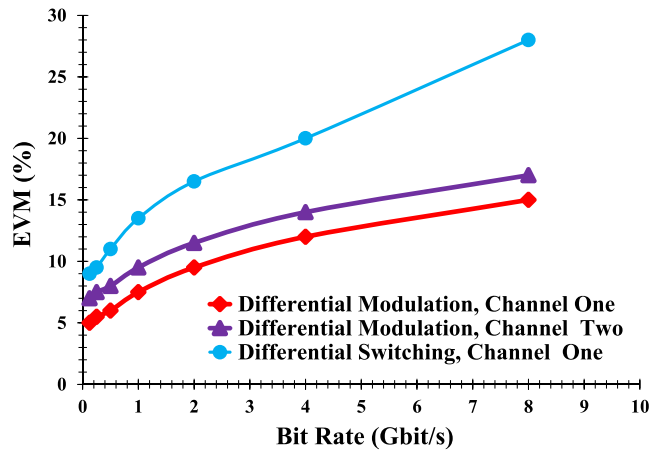


Fig. 11. EVM versus bit rate for frequency down conversion of OFDM modulated data at the mixing frequency of 1 and 2 GHz based on the differential modulation and switching architectures. The simultaneous input data signals at 79 and 80 GHz are down converted at 1 and 2 GHz, respectively for the differential modulation. The input data signal at 79 GHz is down converted at 1 GHz for the differential switching.

Declaration of Competing Interest

The authors declare that they have no known competing financial interests or personal relationships that could have appeared to influence the work reported in this paper.

References

- [1] V.A. Thomas, M. El-Hajjar, L. Hanzo, Millimeter-wave radio over fiber optical upconversion techniques relying on link nonlinearity, *IEEE Commun. Surv. Tutor.* 18 (1) (2016) 29–53.
- [2] H.-J. Song, J.S. Lee, J.-I. Song, Signal up-conversion by using a cross-phase-modulation in all-optical SOA-MZI wavelength converter, *IEEE Photon. Technol. Lett.* 16 (2) (2004) 593–595.
- [3] H.-J. Kim, S.-H. Lee, J.-I. Song, Generation of a 100-GHz optical SSB signal using XPM-based all-optical frequency upconversion in an SOAMZI, *Microw. Opt. Technol. Lett.* 57 (1) (2014) 35–38.
- [4] D.-H. Kim, J.-Y. Lee, H.-J. Choi, J.-I. Song, All-optical single side band frequency upconversion utilizing the XPM effect in an SOAMZI, *Opt. Express* 24 (18) (2016) 20309–20317.
- [5] H. Termos, T. Rampone, A. Sharaiha, A. Hamié, A. Alaeddine, All optical radiofrequency sampling mixer based on a semiconductor optical amplifier Mach-Zehnder interferometer using a standard and a differential configuration, *IEEE J. Lightw. Technol.* 34 (20) (2016) 4688–4695.
- [6] N. Yan, J. del Val Puente, T.G. Silveira, A. Teixeira, A.P.S. Ferreira, E. Tangdiongga, P. Monteiro, A.M.J. Koonen, Simulation and experimental characterization of SOA-MZI-based multiwavelength conversion, *IEEE J. Lightw. Technol.* 27 (2) (2009) 117–127.
- [7] C.K. Sun, R.J. Orazi, S.A. Pappert, W.K. Burns, A photonic-link millimeter-wave mixer using cascaded optical modulators and harmonic carrier generation, *IEEE Photon. Technol. Lett.* 8 (9) (1996) 1166–1168.
- [8] C.S. Park, C.K. Oh, C.G. Lee, D.-H. Kim, C.-S. Park, A photonic up-converter for a WDM radio-over-fiber system using cross-absorption modulation in an EAM, *IEEE Photon. Technol. Lett.* 17 (9) (2005) 1950–1952.
- [9] J. Thouras, B. Benazet, H. Leblond, C. Aupetit-Berthelemot, Photonic radio frequency down-converter based on parallel electro-absorption modulators in Ku/Ku band for space applications, in *Proc. Opto Electron. Commun. Conf./Int. Conf. Photon. Switching, Niigata, Japan, 2016*, pp. 576–578.
- [10] F. Paresys, T. Shao, G. Maury, Y. Le Guennec, B. Cabon, Bidirectional millimeter-wave radio-over-fiber system based on photodiode mixing and optical heterodyning, *IEEE/OSA J. Opt. Commun. Netw.* 5 (1) (2013) 74–80.
- [11] A.W. Mohammad, H. Shams, C.-P. Liu, C. Graham, M. Natrella, A.J. Seeds, C.C. Renaud, 60-GHz transmission link using uni-traveling carrier photodiodes at the transmitter and the receiver, *IEEE J. Lightw. Technol.* 36 (19) (2018) 4507–4513.
- [12] Y.-K. Seo, C.-S. Choi, W.-Y. Choi, All-optical signal up-conversion for radio-on-fiber applications using cross-gain modulation in semiconductor optical amplifiers, *IEEE Photon. Technol. Lett.* 14 (10) (2002) 1448–1450.
- [13] H. Kim, H. Song, J. Song, All-optical frequency up-conversion technique using four-wave mixing in semiconductor optical amplifiers for radio-over-fiber applications, in *IEEE/MTT-S International Microwave Symposium, Honolulu, HI, 2007*, pp. 67–70.
- [14] H.-J. Kim, J.-I. Song, Simultaneous WDM RoF signal generation utilizing an all-optical frequency up converter based on FWM in an SOA, *IEEE Photon. Technol. Lett.* 23 (12) (2011) 828–830.
- [15] H. Termos, T. Rampone, A. Sharaiha, Sampling rate influence in up and down mixing of QPSK and OFDM signals using an SOA-MZI in a differential configuration, *Electron. Lett.* 54 (16) (2018) 990–991.
- [16] D. Kastritsis, T. Rampone, K.E. Zoiros, A. Sharaiha, Modulation and switching architecture performances for frequency up-conversion of complex-modulated data signals based on a SOA-MZI photonic sampling mixer, *IEEE J. Lightw. Technol.* 38 (19) (2020) 5375–5385.
- [17] R.P. Schrieck, M.H. Kwakernaak, H. Jackel, H. Melchior, All-optical switching at multi-100-Gb/s data rates with Mach-Zehnder interferometer switches, *IEEE J. Quantum Electron.* 38 (8) (2002) 1053–1061.
- [18] M. Spyropoulou, N. Pleros, A. Miliou, SOA-MZI-based nonlinear optical signal processing: a frequency domain transfer function for wavelength conversion, clock recovery, and packet envelope detection, *IEEE J. Quantum Electron.* 47 (1) (2011) 40–49.
- [19] **VPI Transmission maker/VPI component maker, User's Manual, Photonic Modules Reference manuals.**
- [20] R. Schmogrow, B. Nebendahl, M. Winter, A. Josten, D. Hillerkuss, S. Koenig, J. Meyer, M. Dreschmann, M. Huebner, C. Koos, J. Becker, W. Freude, J. Leuthold, Error vector magnitude as a performance measure for advanced modulation formats, *IEEE Photon. Technol. Lett.* 24 (1) (2012) 61–63.
- [21] M.A. Mestre, H. Mardoyan, C. Caillaud, R.R. Muller, J. Renaudier, P. Jenneve, F. Blache, F. Pommereau, J. Decobert, F. Jorge, P. Charbonnier, A. Konczykowska, J.-Y. Dupuy, K. Mekhazni, J.-F. Paret, M. Faugeron, F. Mallecot, M. Achouche, S. Bigo, Compact InP-based DFB-EAM enabling PAM-4 112 Gb/s transmission over 2 km, *IEEE J. Lightw. Technol.* 34 (7) (2016) 1572–1578.
- [22] H. Termos, T. Rampone, A. Sharaiha, A. Hamié, OFDM Signal Up and Down Frequency Conversions by a Sampling Method Using a SOAMZI, in *International Conference on Microelectronics (ICM), 2017*.